Compressive strength and microstructure evolution of lime-treated silty soil subjected to kneading action

Geetanjali Das, Andry Razakamanantsoa, Gontran Herrier, Dimitri Deneele

Compressive strength and microstructure evolution of lime-treated silty soil subjected to kneading action

Geetanjali Das[a,*], Andry Razakamanantsoa[a], Gontran Herrier[b], Dimitri Deneele[a,c]

[a]*GERS-GIE, Université Gustave Eiffel, IFSTTAR, F-44344 Bouguenais, France*

[b]*Lhoist Recherche et Développement, rue de l'Industrie 31, 1400 Nivelles, Belgique*

[c]*Université de Nantes, CNRS, Institut des Matériaux Jean Rouxel, IMN, F-44000 Nantes, France*

Highlights

- Behaviours of lime-treated silty soil subjected to kneading compaction are investigated.
- Kneading action enhances better lime-dispersion during soil compaction.
- Proper lime-dispersion contributes to enhanced UCS evolution in the long-term.
- Wet side compacted soil shows enhanced UCS during longer and accelerated curing.
- Accelerated-cured and 7 years in-situ cured soil, both kneaded, show UCS of similar level.

Abstract

Long-term improvement in behaviour of soil subjected to lime treatment depends on the mechanism of its implementation. In-situ lime-treated fine-grained soil is often subjected to 'kneading action' developed by Pad-foot roller. The mechanism underlying the effect of kneading on lime-treated soil remains less investigated. Unconfined Compressive Strength (UCS) and microstructural modification of the lime-treated soil subjected to kneading compaction are evaluated. Kneading action undergoes better lime-dispersion during compaction. This feature accompanied with available water favours the long-term pozzolanic-reactions and hence enhanced the UCS evolution, particularly in the kneaded soil compacted at Wet Moisture Content (WMC). Lime-treated kneaded soil compacted at WMC, which is slightly higher than the Optimum Moisture Content (OMC) is beneficial for enhanced UCS evolution in specimens subjected to longer and accelerated curing. The UCS evolution in the laboratory accelerated-cured kneaded soil is of a similar level as the average UCS measured in the in-situ 7 years atmospherically cured kneaded soil.

Author Accepted Manuscript
Transportation Geotechnics, 29(2021). Elsevier
DOI: 10.1016/j.trgeo.2021.100568

Keywords: lime-treated soil; kneading compaction; Unconfined Compressive Strength; lime-dispersion; pozzolanic-reactions

1. Introduction

Efficient and effective management of natural resources such as soil is essential in any land development project. Thus, several chemical stabilisation processes associated with suitable implementation processes (compaction, soil-mixing, soil-chemical-mixing, *etc*.) are commonly practiced for improving the engineering properties of natural soil. Chemical stabilisation involves the use of inorganic or organic binders, such as slags [1–4], fly ashes produced from coal-burning [5,6], cement kiln dust [7,8], alkaline activator [9,10], lime [11-15], *etc.*

The use of lime in the form of quicklime or hydrated lime is a widespread technique for such improvement. Lime is one of the most versatile [16], low-cost [17], and easily available chemicals. It was shown to be paramount in several applications using environmentally friendly techniques [16]. Soil treated by lime can be used repeatedly, which is another cost-effective measure [18].

Soil improvement by lime consists of two primary modification mechanisms: a) the instant cation exchange reactions and flocculation-agglomeration resulting in a reduction of soil plasticity and improvement of workability, and b) the long-term pozzolanic-reactions leading to the development of the cementitious compounds, thus increasing the soil strength [19–22]. Construction of earth structures such as earth embankments for roads, airports, or railway lines, hydraulic structures, pavement subgrades is successfully implemented because of improvement brought about by lime treatment [11,14,21,23]. One of such examples of earthen hydraulic structures is the Friant-Kern Canal in California, United States. The bottom and blankets of several sections of the canal, initially built with heavy plastic clays, were renovated during the '70s using 4% quicklime by weight [24,25]. Study up to more than 40 years after the renovation was conducted, which showed increased long-term strength, reduction in swelling potential, erosion resistance, thus indicating good geo-mechanical stability of the lime-treated structure [11]. Another study was recently reported by Das et al. [23], where the long-term effect of lime treatment on the mechanical, physicochemical, and microstructural evolution of an embankment constructed and atmospherically cured for 7 years were demonstrated. This study showed a significant evolution in average UCS of about 3.29 ± (0.45) MPa due to the development of cementitious compounds because of the long-term pozzolanic reactions. Thus, the durability and reliability of these structures throughout the service life are linked to the hydromechanical performance of the soil.

Several studies have reported that lime treatment increases the permeability of soil due to the flocculation of particles, which increases the inter-aggregates pore space [26-28]. Others have shown that permeability increases at the beginning of treatment and decreases with increased curing due to the evolution of cementitious compounds [29,30]. Makki-Szymkiewicz et al. [14] conducted a permeability study on a 2.5% quicklime treated silty soil experimental embankment for about 6 months from the time of construction. The study reported a similar level of permeability values in the lime-treated and untreated soils over the 6 months of curing, concluding that conducting controlled mixing and compaction conditions during the construction improves the hydraulic performance of lime-treated soil. As a result, the same embankment, after 7 years from construction was also reported to have a uniform distribution of pH and water content by Das et al. [23], which led to a significant evolution in compressive strength. Thus, the long-term hydromechanical performance can be said to be associated with the compaction conditions implemented during the construction of such structures.

Compaction conditions, such as compaction procedure, energy, and compaction water content, were demonstrated to impact the hydromechanical improvement brought by lime treatment in the soil through several controlled laboratory investigations [13,31-39]. Le Runigo et al. [34] and Mitchell et al. [40] stated that lime-treated soil compacted with different initial moisture contents and compaction energies show different magnitudes of initial permeability coefficient, *k*. A greater magnitude of *k* indicates a greater quantity of water percolation through the compacted soil. Water flow could enhance the dissolution of cementitious compounds, consequently decreasing the UCS of the lime-treated soil [13,32,34,36]. This is because *k* of a soil depends on the pore size distribution (PSD) of the soil, which was shown to be a direct function of compaction conditions by several studies [41–43]. However, how well the above laboratory conditions represent the realistic field conditions is still an important question.

On the field, the usual design-construct of an earthwork project is as follows: The proposed soil materials are initially subjected to a laboratory test to define the compaction parameters required for the design. During the construction, these compaction parameters are achieved by implementing the compaction procedure, which is often adjusted according to the type of soil. All soil types except for rocky soil are compacted by Smooth-wheeled roller [44], while fine-grained soil, particularly clayey soil, is preferred to be compacted by Padfoot roller [45-47]. Lekarp et al. [48] demonstrated that Smooth-wheeled roller develops two types of compaction mechanisms in the soil, *i.e.*, generation of stress tensors at the point of contact of the roller and the soil and a continuous rotation of these stress tensors due to the cyclic passes of the roller wheel. However, Padfoot roller, in addition to the rolling action of the wheel, produces a kneading action by the pad foot present on the drum surface of the roller. Thus, penetration of the pads occurs in the soil during compaction [47,49].

Though the effect of roller compaction was detailed by Lekarp et al. [48], and recently its implementation was shown in le Vern et al. [50], the effect of kneading action has not been well investigated. Clegg [51] urged the importance of implementing kneading compaction at a laboratory scale to produce realistic laboratory compacted fine-grained specimens by showing a similar generation of soil structure and residual interparticle stresses with the in-situ soil. Kouassi et al. [45] confirmed that soil properties, including the dry density and elastic stiffness obtained under kneading effect at a laboratory scale, were close to those obtained in the in-situ compacted soil. Cuisinier et al. [31] and Herrier et al. [24] highlighted that the magnitude of *k* obtained from kneaded lime-treated silty soil was lower compared to the soil compacted statically.

However, apart from these studies, the effect of kneading compaction on mechanical behaviour is less investigated. The consideration of compaction energy is not available in the previous studies, which is essential to analyse the soil mechanical behaviour. Moreover, since kneading compaction was shown to bring a difference in *k,* which correlates with microstructural characteristics, the contribution of the kneading effect to the mechanical behaviour must be evaluated.

In this context, the present study investigates how the kneading mechanism contributes to the mechanical performance and microstructural modifications of lime-treated soil at a laboratory scale. The first section of the study highlights the compressive strength of kneaded soil by comparing the same with soil compacted by a reference standard method. The second section describes the contribution of kneading compaction at microstructure levels. Finally, comments are made on how the generation of mesopores because of lime treatment contributes to the evolution of UCS.

2. Materials and Methodologies

2.1. Soil and Lime properties

The material used in this study is silty soil. Details regarding the geotechnical properties of the soil were obtained from the study reported by Makki-Szymkiewicz et al. [14]. The soil was composed of 12% clay content, 82% silt fraction, and the content of soil passing through 80 µm sieve was 99.5%. The liquid limit and plasticity index of the soil was 31% and 11%, respectively. The Methylene value was 2.5 g/100 g. The mineralogy of the soil, obtained by X-ray diffraction, showed the presence of Illite, Kaolinite, and Chlorite as clay minerals along with Quartz and Feldspars [15].

The quicklime (CaO) used for the treatment was supplied by a commercial supplier. The lime consists of 90.9% of available CaO and a reactivity (t_{60}) of 3.3 min. The Lime Modification Optimum

(LMO) of the silt, which defines the minimum lime content required to initiate the pozzolanic-reactions [52], was determined by Eades and Grim test as per the ASTM D 6276-99a [53]. The LMO was found to be 1% by weight of lime. Three different lime contents were used, lime content equal to LMO, 2.5%, and 4%.

2.2. Sample preparations

The maximum dry density, $\rho_{d(max)}$, and OMC of the silt obtained as per the standard Proctor compaction test mentioned in ASTM D698-91 [54] are presented in Table. 1. Once the characteristics of compaction were deduced, the silt was then air-dried and sieved using 5 mm-sieve. Soil mixtures for both the kneading and static compaction were prepared at OMC (Table 1) and the wet of OMC, i.e., at WMC (= 1.1 × OMC) and stored in sealed plastic bags for about 24 hours to attain moisture content homogenization. Thus, the initial compaction characteristics (Table 1) of the soil mixture subjected to both types of compactions were kept constant. The wet soil and the respective lime were then mixed and rested for 1 hour before compaction. This above process of soil preparation was as per the procedure mentioned in the French GTS Technical Guide for soil treatment [55], which is also a reference for in-situ construction of lime-treated structures.

Table 1

Maximum dry density and OMC of untreated and lime-treated silty soil using Standard Proctor test

Soil	$\rho_{d(max)}$ (kN/m^3)	OMC (%)
Untreated silty soil	18.4	14.3
Silty soil treated with 1% lime	17.4	17.6
Silty soil treated with 2.5% lime	17.1	18.5
Silty soil treated with 4% lime	17.0	18.7

Cylindrical specimens of dimensions having a length of 10cm and a diameter of 5cm were prepared by both kneading and static compactions. The static compaction involves compression of the specimens from top and bottom, as demonstrated by Holtz et al. [44]. This was considered as the standard reference compaction method.

In this study, the kneading compaction was conducted by a laboratory-developed kneading tool, which was equipped with a dynamic load, as presented in Fig. 1. The application of the dynamic load was

made successively with the rotation of the 3-kneading feet by an angle of 45° between 2 successive loadings. This procedure was demonstrated by Kouassi et al. [45]. The applied compaction energy was adjusted as recommended by ASTM D698-91 (Equation 1).

$$E = \frac{N \times H \times n \times m \times g}{V} \quad (1)$$

where, E is the compaction energy (kN-m/m³); N = 16, which is the number of blows per layer; H = 0.14 m, i.e., the height of the falling load; n = 5, the number of compacted layers; m = 1.042 kg, the mass of the falling load (kg), g = acceleration due to gravity (m/s²), V = 187 cm^3 i.e., the volume of the mould.

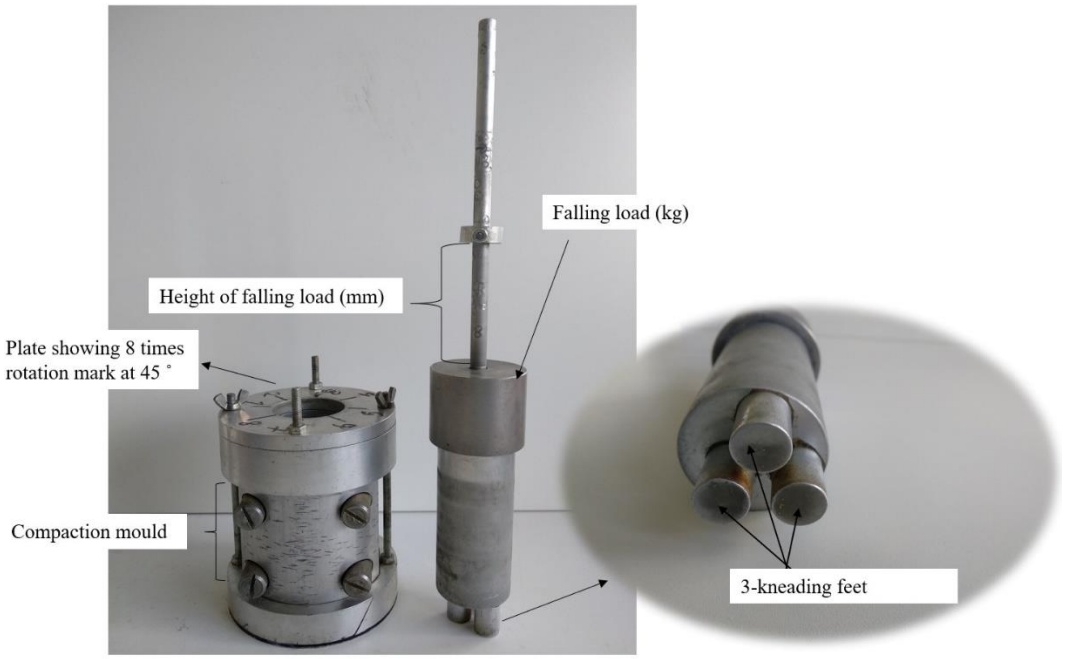

Fig. 1. Laboratory Kneading Compaction tool

After compaction, the bulk density of each specimen was evaluated. The average bulk density of all the kneading and statically compacted specimens was 20.0 kN/m^3 and 19.7 kN/m^3, respectively. Thus, the average bulk density obtained using both compaction methods was similar. Hence, the precision of the kneading tool developed in the laboratory in achieving the targeted bulk density (*i.e.*, obtained from the standard static tool) can be justified.

A total of 72 specimens, including duplicates for each soil configuration, were prepared for strength and microstructural investigations by both compaction methods (Table 2).

Table 2

Types and number of specimens prepared by static-and kneading-compactions

Compaction modes	Curing conditions		Compaction moisture content	Lime contents	Number of specimens (including duplicates)
	Curing time (days)	Curing temperature (°C)			
Static	28	20	OMC	1%, 2.5%, 4%	6
			WMC		6
	90		OMC	1%, 2.5%, 4%	6
			WMC		6
	180	40	OMC	1%, 2.5%, 4%	6
			WMC		6
Kneading	28	20	OMC	1%, 2.5%, 4%	6
			WMC		6
	90		OMC	1%, 2.5%, 4%	6
			WMC		6
	180	40	OMC	1%, 2.5%, 4%	6
			WMC		6

Forty-eight of the total specimens were cured for 28- and 90-days at a laboratory temperature of about 20˚C, and the remaining were cured for 180 days at 40°C, *i.e.*, under accelerated curing (Table 2). After curing, specimens prepared for microstructural analysis were freeze-dried and then stored in vacuum bags to avoid atmosphere interactions until further analysis.

The following nomenclature is used for specimen's identification: lime content (1/2.5/4)-Static compaction method/Kneading compaction method (S/K)-compaction moisture content (OMC/WMC)-curing time (28/90/180) days. For example, 1-K-OMC-28 means 1% lime-treated soil subjected to kneading compaction (K) at OMC and then cured for 28 days.

2.3. Laboratory tests

After curing, specimens were subjected to UCS test using a mechanical press with a load sensor at a constant displacement rate of 1mm/min.

Pore characterization was made by Mercury Intrusion Porosimetry (MIP) test and Barrett-Joiner-Halenda pore (BJH) method [56] on freeze-dried specimens. The motive behind operating both these methods was to investigate the influence of lime treatment on pore structure modifications more elaboratively. MIP is generally used for macropore investigation [23,57,58], while BJH for measuring mesopores and micropores [23,59].

The procedure of MIP test involves the evacuation of freeze-dried samples via heating inside a sealed penetrometer. Mercury was then progressively introduced into the samples through incremental hydraulic pressure. The volume of mercury intruded, and the applied pressure, p (MPa), was registered [60]. By measuring the pressure p required to be applied to force the mercury into a cylindrical pore of diameter, *D*, pore sizes can be obtained according to the Washburn equation (Equation 2) [60].

$$D = \frac{4.\gamma.\cos\theta}{\mathrm{p}} \qquad (2)$$

D is the diameter of the entrance pore where mercury intrudes, γ is the surface tension of mercury, and θ represents contact angle.

The BJH method involves analysing pore structure from the isotherms obtained by Brunauer-Emmett-Teller (BET) test [61], which uses nitrogen gas. Freeze-dried samples were evacuated or degassed at 50°C. Nitrogen gas at temperature, T of 77K, and pressure (p) lower than the equilibrium/saturation gas pressure (p_0) was then injected. Pore structure is determined by using the Kelvin equation (Equation 3) [62].

$$r_k = \frac{2.V_m.\gamma.\cos\theta}{\mathrm{R.T.ln}\left(\frac{p}{p_0}\right)} \qquad (3)$$

where r_k is the radius of curvature of the condensed gas inside the pore, γ is the surface tension, V_m is the molar gas volume of an ideal gas, θ is the contact angle, and R is the gas constant. In this study, the pore structure analysed by BJH was presented in the form of isotherm plots and cumulative mesopore volume. The cumulative mesopore volume corresponding to the desorption branch of isotherm was used.

The discussion related to pore classifications was made as per the International Union of Pure and Applied Chemistry (IUPAC) [63], which classifies pores based on their pore-width as macropores (> 500 Å), mesopores (20-500 Å), and micropores (< 20 Å).

Calcium distribution evolution considering the Ca-mapping was shown to be a useful approach to observe the distribution of lime in lime-treated soil by Lemaire et al. [64]. In this aspect, the µ-XRF images are recorded for lime-treated kneading and statically compacted specimens to assess the effect of compaction on the lime-dispersion. The µ-XRF analysis was performed on freeze-dried specimens, impregnated with polyester resin (LR White ©), and polished with ethanol. The device used equipped with a rhodium RX source and an EDS system (using an SDD detector). Chemical maps of 2 mm square sample sections were recorded.

The observed distribution of calcium was then quantitatively analysed by using imaging software NIS-Elements Basic Research 3.1.

3. Results

3.1. UCS of kneading compacted specimens

Fig. 2 presents the trend of strength evolution in the lime-treated kneading compacted specimens subjected to different curing periods and temperatures. The presentation was made in terms of the average stress-strain obtained from duplicates of each soil configuration. The UCS value, representing the peak of the stress-strain curve, is presented in Table 3.

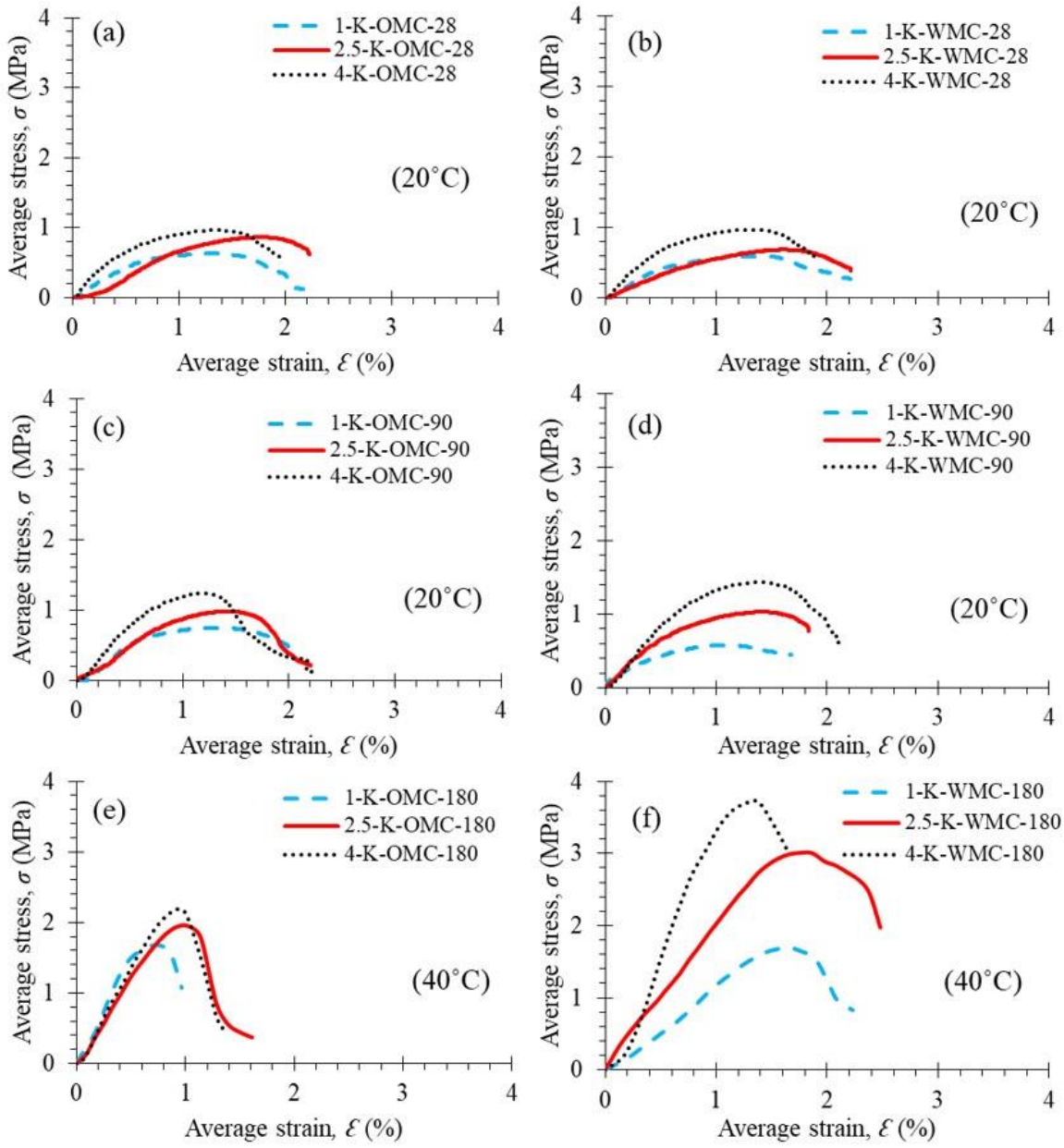

Fig. 2. Strength evolution of 1%, 2.5% and 4% lime-treated kneading compacted specimens at OMC-28 days (a), WMC-28 days (b), OMC-90 days (c), WMC-90 days (d), OMC-180 days (e), and WMC-180 days (f)

Table 3

UCS measured in lime-treated kneaded soil subjected to different curing time and temperatures

	OMC-compacted specimens	WMC-compacted specimens

Lime content (%)	Curing time (days)	Curing temperature (°C)	UCS (MPa)	UCS (MPa)
1	28	20	0.60	0.60
	90	20	0.75	0.60
	180	40	1.70	1.70
2.5	28	20	0.86	0.70
	90	20	1.00	1.03
	180	40	1.95	3.00
4	28	20	0.96	1.20
	90	20	1.23	1.43
	180	40	2.20	3.70

The UCS of the lime-treated kneading compacted soil increased with the increase in lime content and curing time, as seen in Table 3 and Fig. 2. This increase in UCS was significantly higher for the accelerated cured specimens after 180 days of curing compared to the increase in UCS from 28 to 90 days of curing at 20˚C.

Besides, the evolution of UCS was relatively higher in the WMC-compacted specimens than the corresponding OMC-compacted specimens treated with lime content higher than the LMO. The UCS measured was about 3% and 16% higher for 2.5% and 4% lime-treated specimens, respectively, for the 90-days cured WMC-compacted specimens (Fig. 2d). Similarly, the UCS was about 50% and 70% higher for the 2.5% and 4% lime-treated accelerated cured specimens, respectively, compacted at WMC (Fig. 2f).

3.2. Comparison of UCS evolution

The UCS measured from the kneaded soil, were plotted against the respective values obtained from the standard statically compacted specimens in Fig. 3. Comparisons are made between specimens prepared at the same compaction water content, lime content and subjected to similar curing conditions.

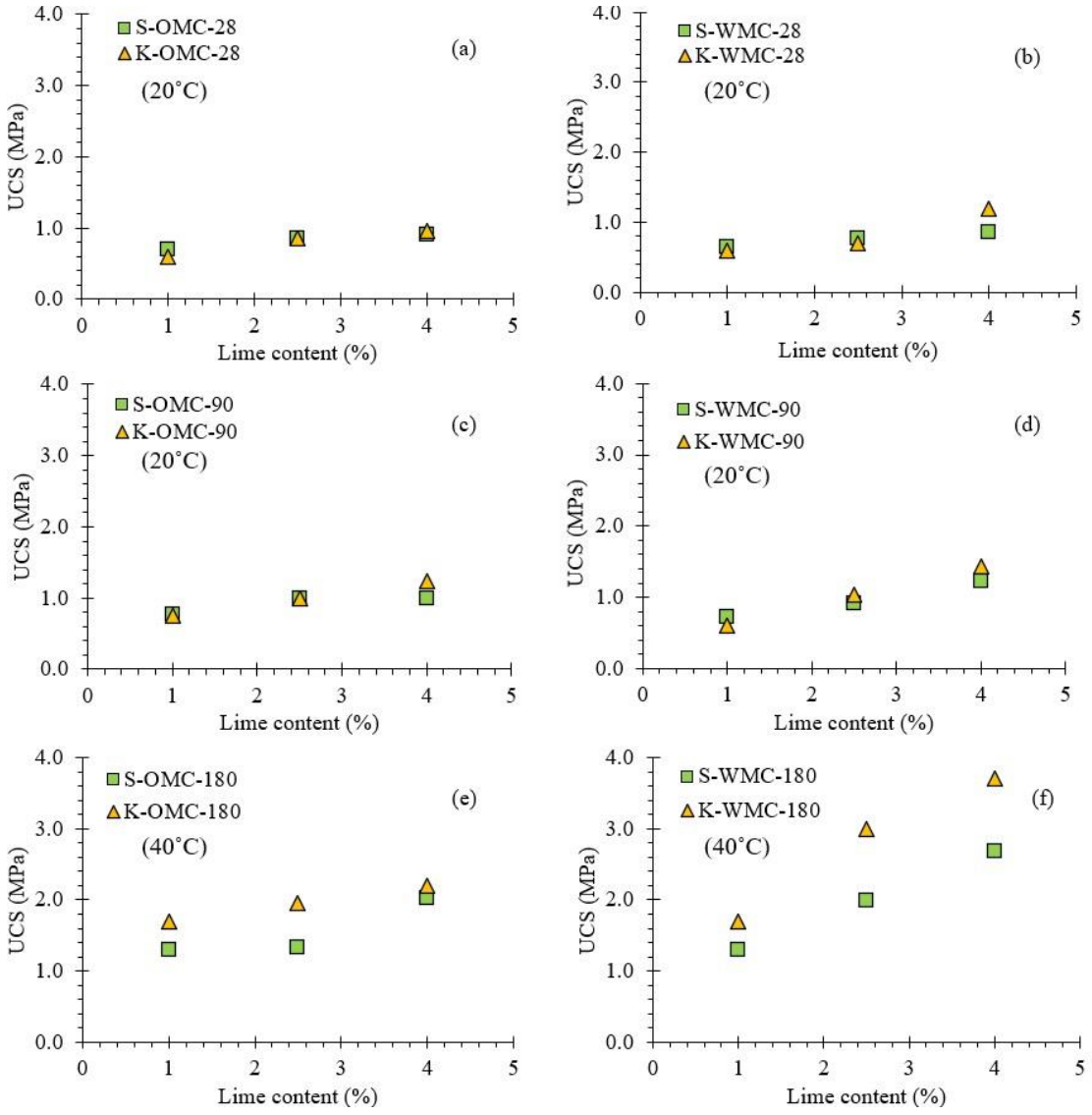

Fig. 3. UCS measured from 1%, 2.5% and 4% lime-treated specimens subjected to static and kneading compactions at OMC-28 days (a), WMC-28 days (b), OMC-90 days (c), WMC-90 days (d), OMC-180 days (e), and WMC-180 days (f)

According to Fig. 3a-d, almost an equivalent UCS level was observed for all the 1% lime-treated compacted specimens, subjected to 28- and 90-days of curing at 20˚C. However, this UCS was about 30% higher in kneaded specimens subjected to accelerated curing (Fig. 3e & f).

For the 2.5% lime-treated OMC-compacted specimens, the UCS level was similar for the 28- and 90-days cured specimens (Fig. 3a & c) and increased by about 45% in the accelerated kneaded specimen (Fig. 3e). For the corresponding WMC-compacted specimens, this UCS level remains almost the same after 28 days of curing (Fig. 3b); increased slightly in the kneaded soil after 90 days of curing (Fig. 3d), and increased by about 50% for the accelerated kneaded specimen (Fig. 3f).

At 4% lime treatment, all the kneaded specimens show about 6-40% greater UCS values.

3.3. Comparison of microstructural modifications

3.3.1. Pore size distribution by MIP

Fig. 4 presents the pore size modification brought by lime treatment in the untreated statically compacted specimens by MIP analysis. As expected, a significant decrease in the pores present at 10^5 and 10^4 Å and evolution of pores lower than 3000 Å was brought on lime additions. Such evolution was also reported by Cuisinier et al. [31]. Besides, the evolution of pores lower than 3000 Å was enhanced with increased lime contents due to the increased formation of cementitious compounds [23,31].

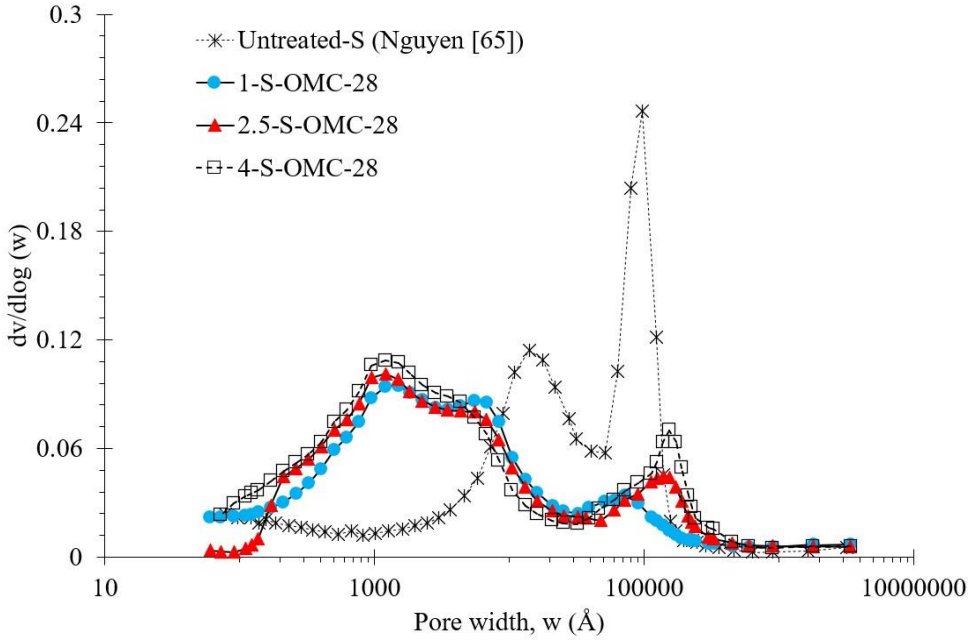

Fig. 4: Evolution of pore structure after addition of 1%, 2.5%, and 4% lime in the untreated statically compacted specimens at OMC and after 28 days of curing

The evolution of pore structures in the lime-treated soil compacted by kneading- and static-compactions at different lime contents were compared in Fig. 5. The comparison was presented in terms of PSD for the OMC- and WMC-compacted 28 days cured and WMC-compacted 90 days cured specimens.

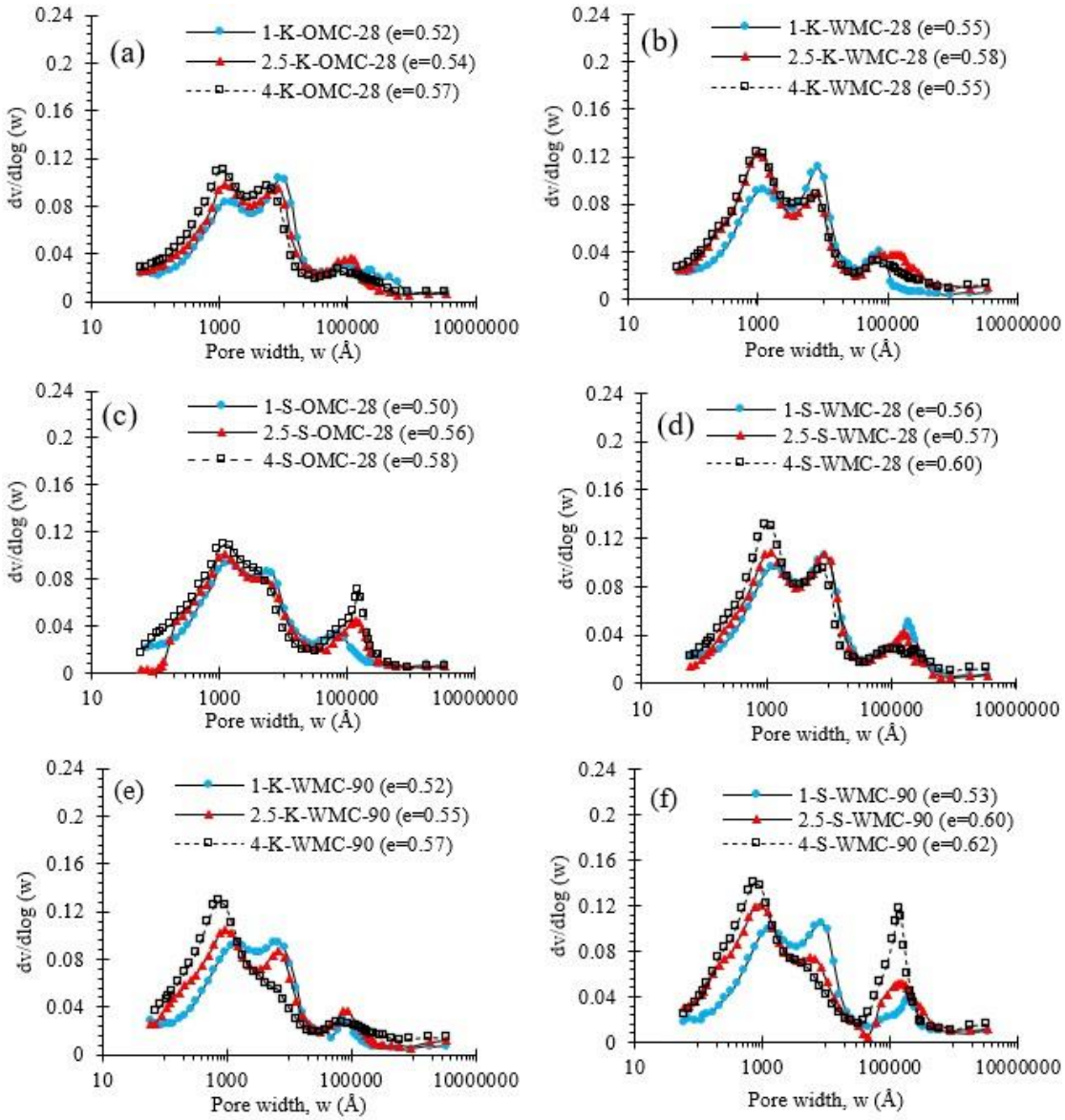

Fig. 5. Analysis of pore structure by MIP for 1%, 2.5% and 4% lime-treated specimens compacted by kneading and static compaction at OMC, and WMC and after 28 days (a-d) and 90 days (e, f) of curing at 20˚C

A small number of macropores of pore diameter 10^5 Å were observed in all three different lime-treated kneaded specimens compacted at both OMC and WMC (Fig. 5a, b & e). On the other hand, for the statically compacted specimens, an increase in the intensity of macropores of pore diameter 10^5 Å was observed with the increased lime content (Fig. 5c, d & f).

Besides, almost a similar decrease in the presence of macropores of diameter 10^4 Å and increased intensity of pores of diameter lower than 3000 Å was observed in both types of compacted specimens, with increase lime content and curing time (Fig. 5a-f).

317

318

319 *3.3.2. Pore size distribution by BJH*

320 Fig. 6 & 7 presents the pore structure analysis by the BJH method in terms of the generation of
321 isotherms and cumulative pore volume evolutions, respectively, in the lime-treated kneading and statically
322 compacted specimens.

323

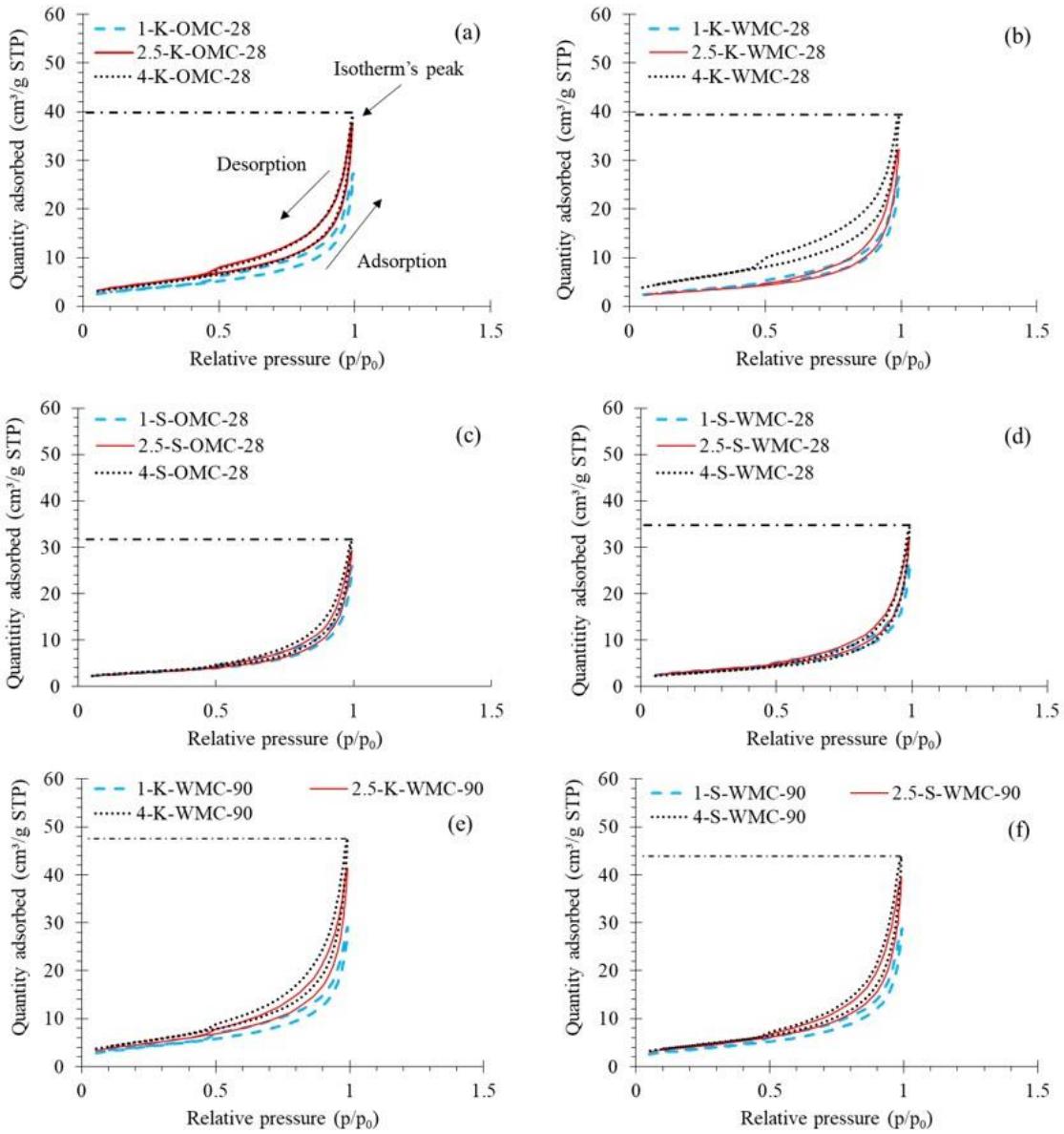

324

325 **Fig. 6**. Evolution of isotherms in 1%, 2.5%, and 4% lime-treated OMC, and WMC kneading and statically compacted specimens
326 after 28 days (a-d) and 90 days (e, f) of curing at 20˚C

The peak of the isotherms, as seen in Fig. 6a, represents the total nitrogen adsorption capacity of the soil [66]. In the analysis made with the present soil, the PSD analysed by the BJH method was found to be in the range of pore diameter of about 20-2000 Å. Thus, the higher is the peak of the isotherm, the greater is the presence of pores of diameter 20-2000 Å in the soil.

Fig. 6 shows that the peak of the isotherm rises with increased lime content. However, this rise was relatively more significant in the 4% lime-treated kneaded soil (Fig. 6a, b & e) than the corresponding rise in statically compacted soil (Fig. 6c, d & f).

The hysteresis developed in the isotherm was relatively distinctive in the 4% lime-treated 28 days cured kneaded soil (Fig. 6a & b). This hysteresis was demonstrated to be associated with the delay in capillary condensation and evaporation that occurs in the mesopores by McGregor et al. [67] and Collet et al. [68]. Thus, an enhanced hysteresis indicates the presence of a greater volume of mesopores [69].

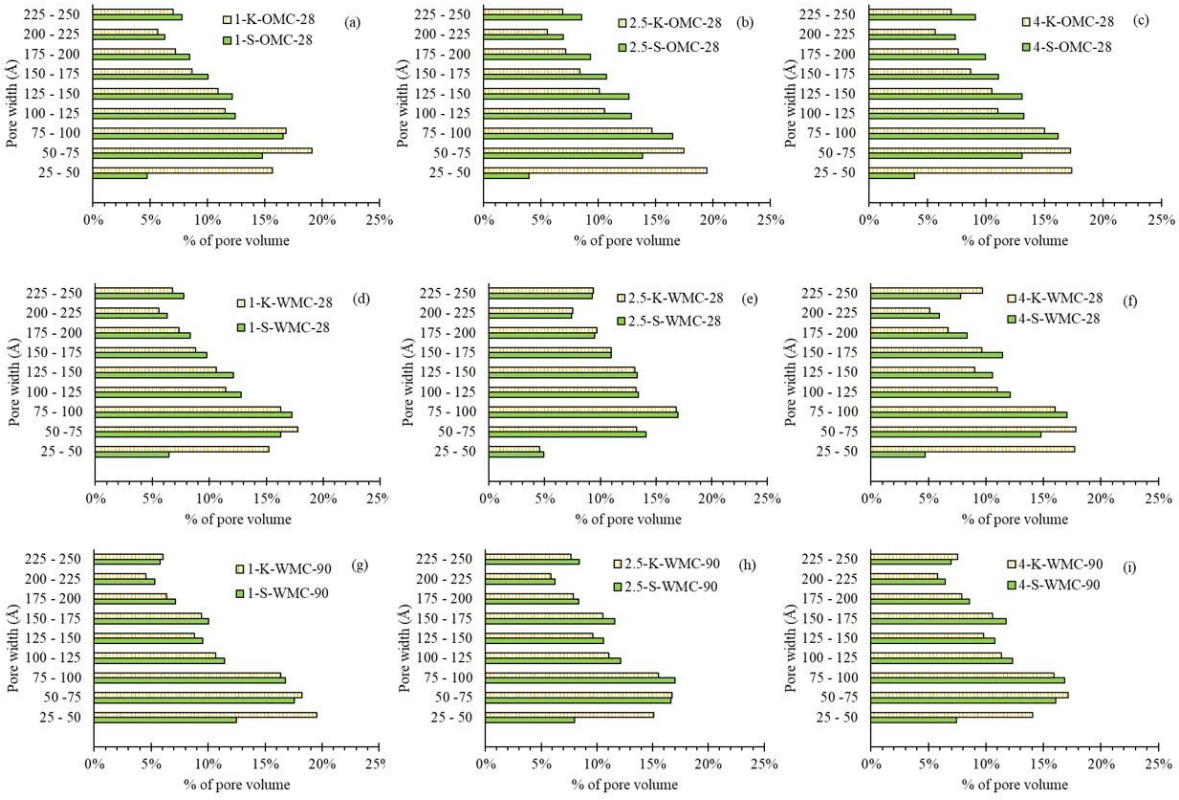

Fig. 7. Percentage of cumulative mesopores volume measured in 1%, 2.5%, and 4% lime-treated OMC, and WMC kneading and statically compacted specimens after 28 days (a-f) and 90 days (g-i) of curing at 20˚C

The cumulative mesopore volume measured in the lime-treated compacted soil was in the range of mesopore diameter 25-250 Å. The variation of these mesopore volumes is presented in terms of the

percentage of mesopore volume for a different interval of mesopore range (Fig. 7). It was observed that almost all the statically compacted soil exhibited a greater percentage of mesopore volume in the range of pore diameter of 100-250 Å. At the same time, the percentage of pore volume was relatively higher in the kneaded soil in the mesopore range of pore diameter lower than 100 Å, i.e., 25-75 Å.

3.3.3. µ-XRF images

Fig. 8 presents the distribution of calcium within the lime-treated soil matrix compacted at OMC and after 28 days of curing. The calcium distribution is represented by the blue region, while soil by the black region. The quantitative analysis of this calcium distribution is presented in Table 4.

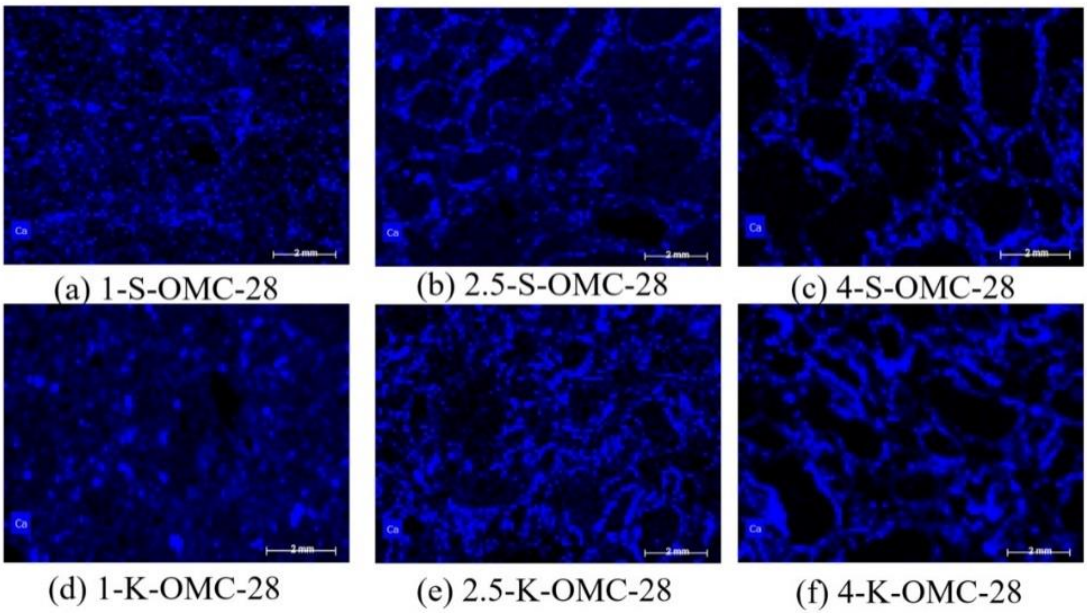

Fig. 8. µ-XRF image highlighting calcium distributions in 1%, 2.5%, and 4% lime-treated static (a, b, & c) and kneading compacted (d, e, & f) specimens prepared at OMC after 28 days of curing time at 20˚C.

Table 4

Percentage distribution of Calcium (Ca) within the polished surface area of the kneading- and statically-compacted specimens

28 days cured specimens

		Kneading compacted	Statically compacted
Lime%-W.C[1]	TSA[2] ($\times 10^{-12}$) (m^2)	% of T.S.A covered by Ca	% of T.S.A covered by Ca
1-OMC	6.0	17.2	13.3
2.5-OMC	7.0	25.4	17.0
4-OMC	6.0	24.4	17.0

[1]*W.C: compaction moisture content*

[2]*T.S.A: Total Surface Area*

Table 4 highlights that, for a constant surface area, the percentage of calcium distribution was about 4 to 8% higher in the lime-treated kneaded specimens than the corresponding statically compacted specimens.

4. Discussion

As expected, kneading compacted soil showed a rise in UCS with increased curing time and lime content (Fig. 2). The significant UCS evolution for the accelerated cured specimens was attributed to the acceleration of pozzolanic-reactions, as demonstrated by Lemaire et al. [64] and Verbrugge et al. [70] (Fig. 2e & f). At the same time, for soil treated with 2.5% and 4% lime, the UCS obtained was relatively higher for the WMC-compacted 90 days cured specimens when compared to the corresponding OMC-compacted specimens (Fig. 2c & d). This increase in UCS was more significant for all the accelerated cured WMC-compacted specimens (Fig. 2e & f). Thus, kneaded soil, treated at lime content higher than LMO, cured for a longer time, and under accelerated condition, shows enhanced UCS in WMC-compacted specimens when compared to OMC-compacted specimens. However, the literature has shown that lime-treated soil compacted at WMC, which is much higher than the OMC and cured for a shorter period, resulted in lower UCS than OMC-compacted soil due to the loss in soil grain-to-grain contact with increased water content [13,71-73]. In the present case, the soil treated at WMC is only 1.1 times higher than OMC and cured for a longer time and under accelerated conditions. Thus, the generation of enhanced UCS in the WMC-compacted specimens indicates an appropriate availability of water in the soil matrix, which might have regulated a steady consumption of water by quicklime for the formation of cementitious compounds with increased curing time and under accelerated conditions. Thus, compacting lime-treated soil at WMC slightly higher than OMC is beneficial for long-term evolution of UCS.

On comparing the dispersion of calcium measured from the polished surface area of the compacted specimens in Fig. 8, it was observed that this dispersion was enhanced under kneading compaction. The percentage of the polished area covered by calcium was about 8% higher in the 2.5%, and 4% lime-treated OMC kneaded specimens compared to the corresponding statically compacted specimens (Table 4). The observed calcium can either be the calcium from the available lime or the cementitious compounds developed because of pozzolanic-reactions. This provides evidence that kneading action enhances lime-dispersion. This feature of enhanced lime dispersion, accompanied by water availability, would contribute to the enhanced pozzolanic-reactions, particularly in the long-term. Thus, kneading compaction acts in favour of pozzolanic-reaction, which consequently leads to better development of cementitious compounds. This was confirmed by a relatively greater generation of mesopores of diameter 20-2000 Å as indicated by the enhanced isotherm peak, by the hysteresis developed (Fig. 6), and by the presence of a greater percentage of mesopore volume in the pore range 25-75 Å (Fig. 7). Increased development of cementitious compounds can increase the overall stiffness of the kneaded soil. This explains the relatively greater UCS obtained in all the 4% lime-treated kneaded soil (Fig. 3), in the 2.5% lime-treated 90 days cured kneaded soil, compacted at WMC (Fig. 3d), and in all the lime-treated accelerated cured kneaded soil (Fig. 3e & f).

Kneading effect was shown to bring more significant deformation in the natural soil aggregates compared to statically compacted specimens by Mitchell and McConnell [38]. Thus, upon kneading compaction of the lime-treated soil at OMC/WMC, a greater aggregate deformation accompanied by enhanced lime-dispersion occurred in comparison to the one that was statically compacted. Such a phenomenon lowered the availability of macropores of diameter 10^5 Å (Fig. 5a, b & e) and enhanced the mesopores evolutions (Fig. 6 & 7) in the kneaded soil. At the same time, macropores of diameter 10^5 Å increased with lime content in the statically compacted specimens (Fig. 5c, d & f), which was due to the formation of greater inter-aggregate pores at higher lime content, as reported by Tran et al. [75] and Wang et al. [76]. The same specimens after curing and on being subjected to UCS showed failure due to consumption of water for cementitious compounds formation. However, owing to the above-mentioned differences produced in soil structure due to the difference in the effect of compactions, kneaded soil showed a higher ductile failure characteristic during UCS test, as evidenced by the differences in the crack development observed between the lime-treated kneading and statically compacted specimens in Fig. 9. The diagonal and vertical crack developed in the kneaded and statically compacted specimens (Fig. 9a & b) represents the shear and tensile crack, respectively, as reported by Kichou Z [74].

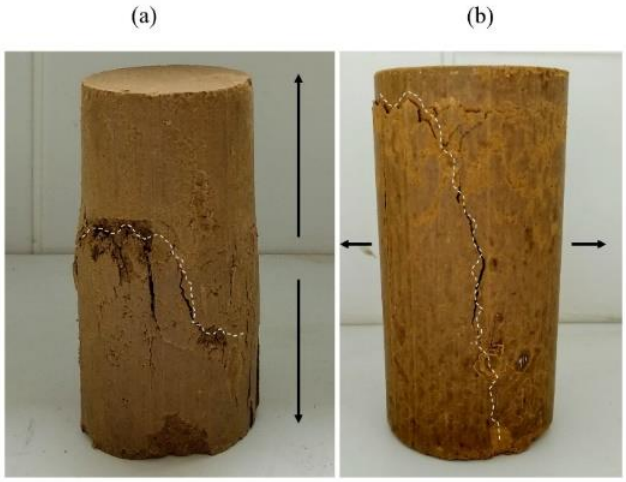

Fig. 9. Diagonal Crack in kneading compacted (a), and vertical crack in statically compacted (b) specimens after UCS test at 1% lime treatment, compacted at OMC and after 28 days curing

Based on the initial findings, the difference in the effect of compaction on aggregates deformation and lime-dispersion in specimens subjected to kneading and static compaction is explained through the schematic diagram presented in Fig. 10.

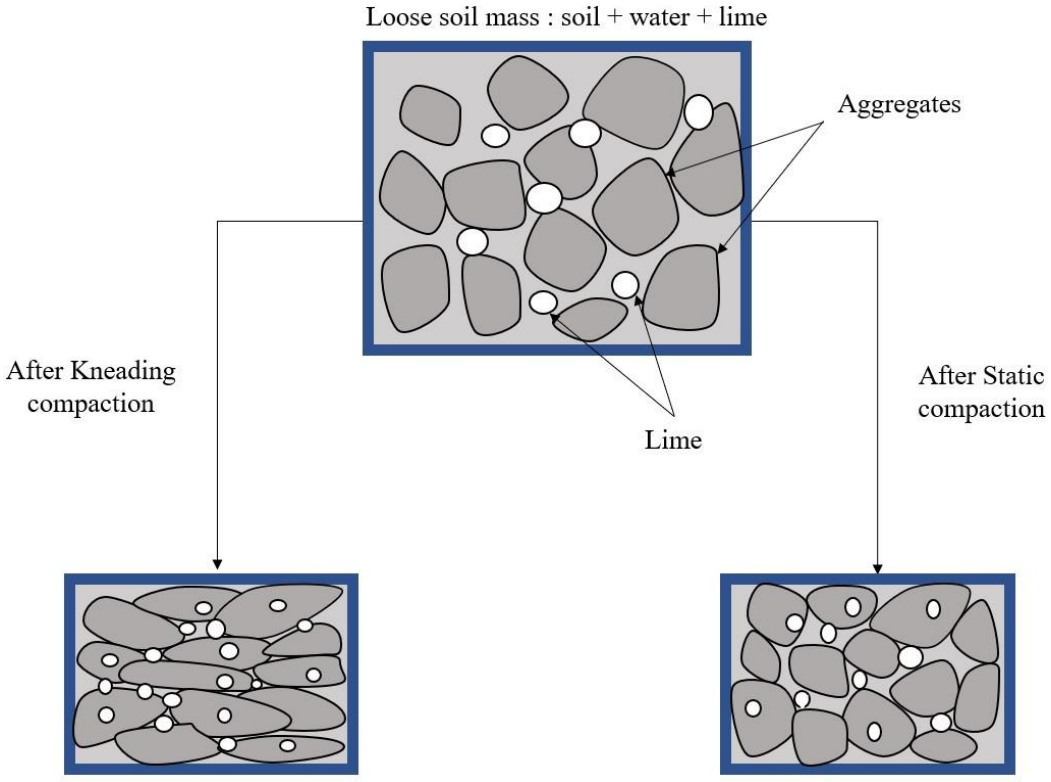

Fig. 10. Schematic diagram showing the difference in the effect of kneading and static compaction on aggregates deformation and lime-dispersion

The present 2.5% lime-treated and WMC-compacted silty soil was used in the construction of an embankment using a vibrating padfoot roller that produces kneading action during compaction [14,72]. The process of construction was as per GTS Technical Guide for soil treatment [55]. After 7 years of atmospheric curing, the embankment was deconstructed, and the UCS of four core-sampled embankment's specimens, namely, T1-1 & T2-4 of length (l)/diameter(d) ratio of both 1 and 2 was evaluated, and the average UCS of these specimens was reported to be 3.29 (± 0.45) MPa [23]. The obtained in-situ UCS was also shown to be repeatable using the correction factor recommended by ASTM-C42-77 [78]. The average UCS of in-situ extracted samples was shown to be comparable with a 90-day laboratory accelerated-cured specimen of similar configuration and of the dimension of l/d=1. The UCS obtained from in-situ and laboratory accelerated cured specimen that has been reported by Das et al. [23] are compared with the trend of UCS obtained with the present accelerated kneaded soil in Fig. 11a & b.

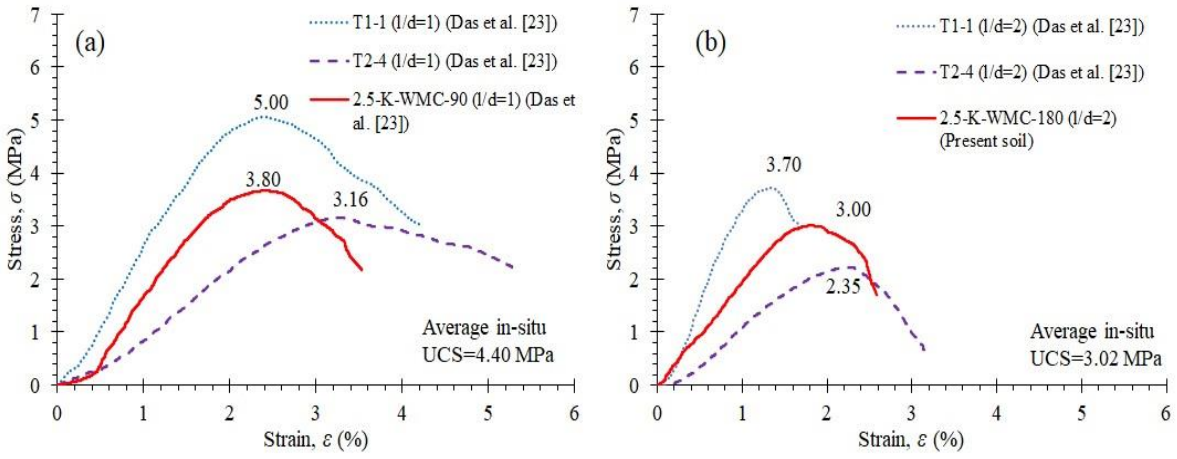

Fig. 11 Comparative evolution of UCS in in-situ core sampled and laboratory-accelerated cured soil of dimension of l/d ratio of 1 (a) and 2 (b).

Fig. 11a & b presents the comparative trend in UCS evolution in the in-situ and laboratory kneaded specimen of dimension l/d=1 and l/d=2, respectively. The average of the in-situ UCS values, if compared with the UCS of the corresponding 2.5% lime-treated accelerated cured laboratory kneaded soil, was found to be of a similar level for both dimensions. The difference in UCS observed between the laboratory 90- and 180-days accelerated cured kneaded specimens was due to the difference in dimension which is in accordance with ASTM-C42-77 [78]. Besides, Das et al. [23] reported that the difference in UCS of the two in-situ cured core-sampled specimens was linked with the intensities of mesopores evolution by BJH.

The mesopore evolution of the present accelerated cured soil was compared with the one obtained from the in-situ cured core sampled kneaded specimens and are presented in Fig. 12.

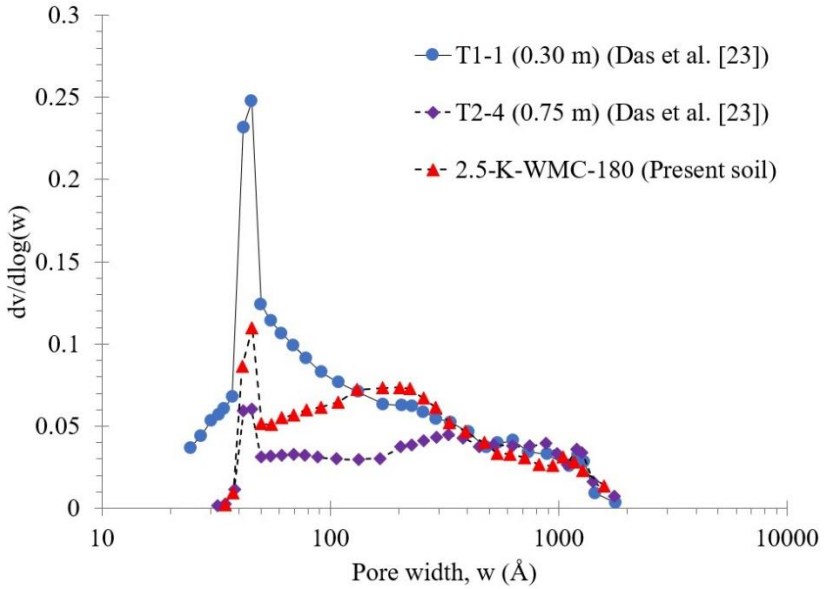

Fig. 12. Comparison of PSD obtained by BJH in 2.5% lime-treated kneaded specimens obtained between laboratory accelerated cured specimen and 7 years in-situ atmospherically cured specimens

Fig. 12 shows that the present accelerated cured kneaded specimen exhibits intensities of mesopores greater than T2-4 and less than T1-1. Thus, the trend observed in the evolution of mesopores between the accelerated-cured and in-situ cured soil, both kneaded, corresponds well with the level of UCS measured. This confirms the fact that the soil cured under laboratory-accelerated condition and the soil sampled after 7 years of environmental exposure, both submitted to kneading action, exhibit a similar level of UCS. This shows evidence of the relevancy of the accelerated condition in the laboratory to access to the long-term UCS level similar to the sample submitted to field condition.

Additionally, Das et al. [23] reported a uniform distribution of pH above 11 and water content throughout the lime-treated embankment after 7 years of atmospheric curing. This evolution was due to the controlled mixing and compaction condition conducted during the construction of the embankment by Makki-Szymkiewicz et al. [14] and Charles et al. [77], which again involves the kneading action due to the use of padfoot rollers. Considering the enhanced dispersive action created by kneading compaction in Fig. 8, a uniform evolution of lime and lime components might have resulted throughout the embankment, thus giving all pH values of the sampled specimens above 11 and a homogeneous water content.

Fig. 4 & 5 showed that lime treatment has led to the generation of pores lower than the pore diameter of 3000 Å, and such generation was shown to increase soil cohesion and enhance UCS by

Verbrugge et al. [70]. However, pores diameter lower than 3000 Å includes a part of macropores, total mesopores, and micropores as per IUPAC (1994). In the present soil, BJH measured the evolution of pores under the lime effect in the range 20-2000 Å (Fig. 6), which includes macropores and mesopores, and the cumulative pore volume in the range 25-250 Å that includes only mesopores (Fig. 7). Hence, to identify the contribution of different classes of pores to the UCS evolution, a regression equation was developed.

The proposed equation (Equation 4) considers compacted specimens cured at 20˚C. The input data of the proposed equation involves the isotherm peak which indicates the total volume of nitrogen injected in pores of diameter 20-2000 Å, and the cumulative pore volume measured in the mesopore range 25-250 Å. The input data is provided in Table 5.

$$UCS = -0.034 + 0.015 \times (\text{pores of diameter 20-2000 Å}) + 27.7 \times (\text{mesopores of diameter 25-250 Å}) \quad (4)$$

Table 5

Isotherm peak and cumulative pore volume measured in lime-treated soil

Samples name	Isotherm peak (cm^3/g)	$^1V_{cum}$ in pore range (25-250 Å) (cm^3/g)	UCS (MPa)	Samples name	Isotherm peak (cm^3/g)	V_{cum} in pore range (25-250 Å) (cm^3/g)	UCS (MPa)
1-K-OMC-28	27.3	0.008	0.60	1-S-OMC-28	26.0	0.011	0.70
2.5-K-OMC-28	37.6	0.015	0.86	2.5-S-OMC-28	29.3	0.013	0.86
4-K-OMC-28	39.3	0.018	1.00	4-S-OMC-28	31.3	0.014	0.90
1-K-WMC-28	26.6	0.010	0.60	1-S-WMC-28	27.0	0.010	0.64
2.5-K-WMC-28	32.2	0.012	0.68	2.5-S-WMC-28	32.0	0.012	0.77
4-K-WMC-28	38.9	0.014	0.96	4-S-WMC-28	34.4	0.012	0.87
1-K-OMC-90	31.4	0.011	0.75	1-S-OMC-90	28.8	0.010	0.77
2.5-K-OMC-90	39.3	0.015	0.98	2.5-S-OMC-90	42.5	0.016	1.00
4-K-OMC-90	46.8	0.020	1.23	4-S-OMC-90	43.0	0.019	1.00
1-K-WMC-90	29.0	0.009	0.60	1-S-WMC-90	28.8	0.011	0.72
2.5-K-WMC-90	41.4	0.017	1.03	2.5-S-WMC-90	39.3	0.016	0.91
4-K-WMC-90	47.7	0.020	1.43	4-S-WMC-90	43.8	0.018	1.23

$^1V_{cum}$: Cumulative pore volume

Equation (4) demonstrates accurately (R^2= 0.90) that the mesopore range 25-250 Å makes the maximum contribution to the rise in UCS in the range of pores lower than 2000 Å developed under the lime effect.

This indicates how lime treatment brings greater development of mesopores due to the cementitious bonding formed because of pozzolanic-reactions and how this contributes towards the strength evolution.

5. Conclusions

The effect of the kneading mechanism on the UCS evolution and microstructural properties of lime-treated silty soil was investigated. Based on the studies, the following findings are derived:

1. Lime-treated kneaded soil, particularly compacted at WMC, prepared at lime content higher than LMO and subjected to longer and accelerated curing, showed enhanced evolution of UCS. With appropriate availability of water in the soil matrix, a steady consumption of water by quicklime was regulated for the formation of cementitious bonding with increased curing time and under accelerated conditions.

2. The kneading action caused relatively greater deformation of large aggregates and decreased the macropores of diameter 10^5 Å, compared to the corresponding statically compacted soil.

3. Kneading compaction enhanced better dispersion of lime during compaction. When accompanied by the available water, such configuration works in favour of long-term pozzolanic-reactions. This resulted in up to about 50% greater UCS in the kneaded soil than the statically compacted soil prepared at lime content greater than LMO, compacted at WMC, and subjected to longer and accelerated curing.

4. The UCS obtained from the laboratory accelerated kneaded soil was of a similar level as the average UCS obtained from in-situ specimens sampled from the 7-year atmospherically cured embankment. The mesopores generation showed a positive trend with respect to the evolution of UCS between the laboratory-accelerated cured, and in-situ cured sampled soil.

5. Increased lime content and curing time resulted in increased isotherm peak, which indicated the greater generation of pores in the range of pore diameter 20-2000 Å. Among the pore ranges produced under the lime effect, the contribution of mesopores in the pore range 25-250 Å towards the evolution of UCS was shown to be most significant, as highlighted by a regression equation relating UCS with pore size.

Thus, the above findings are part of a holistic investigation into the mechanical behaviour and microstructural modification of lime-treated silty soil subjected to kneading action. The kneading action caused compressive strength gain, particularly in the long-term and for WMC-compacted soil. These results were evidenced by UCS and microstructure evaluated from 7 years in-situ cured core-sampled soil. Further

studies are required to be conducted to understand the hydraulic characteristics of lime-treated soil subjected to the kneading effect.

Acknowledgements

This work was financially supported by Association Nationale de la Recherche et de la Technologie with grant N˚2018/0219 and Lhoist Southern Europe with grant N˚RP2-E18114. The authors are very thankful to the research team of Université Gustave Eiffel and Lhoist Nivelles for their great support in performing laboratory experiments and technical supports.

References

[1] Zhou Y, Liu W. Application of granulated copper slag in massive concrete under saline soil environment. Construction and Building Materials 2021; 266:121165. https://doi.org/10.1016/j.conbuildmat.2020.121165

[2] Poh HY, Ghataora GS, Ghazireh N. Soil stabilization using basic oxygen steel slag fines. Journal of Materials in Civil Engineering 2006; 18:229–40 https://doi.org/10.1061/(ASCE)0899-1561(2006)18:2(229)

[3] Wild S, Kinuthia JM, Jones GI, Higgins DD. Effects of partial substitution of lime with ground granulated blast furnace slag (GGBS) on the strength properties of lime-stabilised sulphate-bearing clay soils. Engineering Geology 1998; 51:37–53. https://doi.org/10.1016/S0013-7952(98)00039-8

[4] Bensaifi E, Bouteldja F, Nouaouria MS, Breul P. Influence of crushed granulated blast furnace slag and calcined eggshell waste on mechanical properties of a compacted marl. Transportation Geotechnics 2019; 20:100244. https://doi.org/10.1016/j.trgeo.2019.100244

[5] Kolias S, Kasselouri-Rigopoulou V, Karahalios A. Stabilisation of clayey soils with high calcium fly ash and cement. Cement and Concrete Composites 2005; 27:301–313. https://doi.org/10.1016/j.cemconcomp.2004.02.019

[6] Show K-Y, Tay J-H, Goh ATC. Reuse of incinerator fly ash in soft soil stabilization. Journal of Materials in Civil Engineering 2003; 15:335–43. https://doi.org/10.1061/(ASCE)0899-1561(2003)15:4(335)

[7] Baghdadi ZA, Fatani MN, Sabban NA. Soil modification by cement kiln dust. Journal of Materials in Civil Engineering 1995; 7:218–222. https://doi.org/10.1061/(ASCE)0899-1561(1995)7:4(218)

[8] Miller GA, Azad S. Influence of soil type on stabilization with cement kiln dust. Construction and Building Materials 2000; 14:89–97.https://doi.org/10.1016/S0950-0618(00)00007-6

[9] Wattez T, Patapy C, Frouin L, Waligora J, Cyr M. Interactions between alkali-activated ground granulated blastfurnace slag and organic matter in soil stabilization/solidification. Transportation Geotechnics 2020:100412. https://doi.org/10.1016/j.trgeo.2020.100412

[10] Cristelo N, Glendinning S, Fernandes L, Pinto AT. Effect of calcium content on soil stabilisation with alkaline activation. Construction and Building Materials 2012; 29:167–74. https://doi.org/10.1016/j.conbuildmat.2011.10.049

[11] Akula P, Hariharan N, Little DN, Lesueur D, Herrier G. Evaluating the Long-Term Durability of Lime Treatment in Hydraulic Structures: Case Study on the Friant-Kern Canal. Transportation Research Record 2020; 6: 431-443. https://doi.org/10.1177/0361198120919404.

[12] Bicalho K v, Boussafir Y, Cui Y-J. Performance of an instrumented embankment constructed with lime-treated silty clay during four-years in the Northeast of France. Transportation Geotechnics 2018; 17:100–16. https://doi.org/10.1016/j.trgeo.2018.09.009

[13] le Runigo B, Ferber V, Cui Y-J, Cuisinier O, Deneele D. Performance of lime-treated silty soil under long-term hydraulic conditions. Engineering Geology 2011; 118:20–8. https://doi.org/10.1016/j.enggeo.2010.12.002

[14] Makki-Szymkiewicz L, Hibouche A, Taibi S, Herrier G, Lesueur D, Fleureau J-M. Evolution of the properties of lime-treated silty soil in a small experimental embankment. Engineering Geology 2015; 191:8–22. https://doi.org/10.1016/j.enggeo.2015.03.008.

[15] Nguyen TTH, Cui Y-J, Ferber V, Herrier G, Ozturk T, Plier F. Effect of freeze-thaw cycles on mechanical strength of lime-treated fine-grained soils. Transportation Geotechnics 2019; 21:100281. https://doi.org/10.1016/j.trgeo.2019.100281

590 [16] Dowling A, O'Dwyer J, Adley CC. Lime in the limelight. Journal of Cleaner Production
591 2015; 92:13–22. https://doi.org/10.1016/j.jclepro.2014.12.047

592 [17] Inkham R, Kijjanapanich V, Huttagosol P, Kijjanapanich P. Low-cost alkaline substances for
593 the chemical stabilization of cadmium-contaminated soils. Journal of environmental
594 management 2019; 250:109395. https://doi.org/10.1016/j.jenvman.2019.109395

595 [18] Hopkins TC, Beckham TL, Sun C. Stockpiling Hydrated Lime-Soil Mixtures
596 2007.http://dx.doi.org/10.13023/KTC.RR.2007.12

597 [19] Bell FG. Lime stabilization of clay minerals and soils. Engineering Geology 1996; 42:223–
598 37. https://doi.org/10.1016/0013-7952(96)00028-2

599 [20] Diamond S, Kinter EB. Mechanisms of soil-lime stabilization. Highway Research Record
600 1965; 92:83–102.

601 [21] Little DN. Stabilization of pavement subgrades and base courses with lime. 1995.

602 [22] Rogers CDF, Glendinning S. Modification of clay soils using lime. Lime Stabilisation:
603 Proceedings of the seminar held at Loughborough University Civil & Building Engineering
604 Department on 25 September 1996, Thomas Telford Publishing; 1996, p. 99–114.

605 [23] Das G, Razakamanantsoa A, Herrier G, Saussaye L, Lesueur D, Deneele D. Evaluation of the
606 long-term effect of lime treatment on a silty soil embankment after seven years of atmospheric
607 exposure: Mechanical, physicochemical, and microstructural studies. Engineering Geology
608 2021; 281,105986. https://doi.org/10.1016/j.enggeo.2020.105986

609 [24] Herrier G, Chevalier C, Froumentin M, Cuisinier O, Bonelli S, Fry J-J. Lime treated soil as
610 an erosion-resistant material for hydraulic earthen structures 2012.

611 [25] Knodel PC. Lime in canal and dam stabilization, US Bureau of Reclamation. Report No GR-
612 87-10, 21p; 1987.

613 [26] Khattab A, Suhail A. Etude multi-échelles d'un sol argileux plastique traité à la chaux. PhD
614 diss., Orléans 2002.

615 [27] Rajasekaran G, Rao SN. Permeability characteristics of lime treated marine clay. Ocean
616 Engineering 2002; 29:113–27. https://doi.org/10.1016/S0029-8018(01)00017-8

[28] Nalbantoglu Z, Tuncer ER. Compressibility and hydraulic conductivity of a chemically treated expansive clay. Canadian Geotechnical Journal 2001; 38:154–60. https://doi.org/10.1139/t00-076

[29] Locat J, Trembaly H, Leroueil S. Mechanical and hydraulic behaviour of a soft inorganic clay treated with lime. Canadian Geotechnical Journal 1996; 33:654–69. https://doi.org/10.1139/t96-090-311

[30] Lasledj A. Traitement des sols argileux à la chaux: processus physico-chimique et propriétés géotechniques. PhD diss., Orléans 2009.

[31] Cuisinier O, Auriol J-C, le Borgne T, Deneele D. Microstructure and hydraulic conductivity of a compacted lime-treated soil. Engineering Geology 2011; 123:187–93. https://doi.org/10.1016/j.enggeo.2011.07.010

[32] Deneele D, Le Runigo B, Cui Y-J, Cuisinier O, Ferber V. Experimental assessment regarding leaching of lime-treated silt, Construction and Building Materials 2016; 112:1032–1040. https://doi.org/10.1016/j.conbuildmat.2016.03.015

[33] Dhar S, Hussain M. The strength and microstructural behavior of lime stabilized subgrade soil in road construction. International Journal of Geotechnical Engineering 2019:1–13. https://doi.org/10.1080/19386362.2019.1598623

[34] le Runigo B, Cuisinier O, Cui Y-J, Ferber V, Deneele D. Impact of initial state on the fabric and permeability of a lime-treated silt under long-term leaching. Canadian Geotechnical Journal 2009; 46:1243–1257. https://doi.org/10.1139/T09-061

[35] Rosone M, Celauro C, Ferrari A. Microstructure and shear strength evolution of a lime-treated clay for use in road construction. International Journal of Pavement Engineering 2020; 21:1147–1158. https://doi.org/10.1080/10298436.2018.1524144

[36] Cuisinier O, Deneele D, Masrouri F. Shear strength behaviour of compacted clayey soils percolated with an alkaline solution. Engineering Geology 2009; 108:177–188. https://doi.org/10.1016/j.enggeo.2009.07.012

[37] Daniel DE, Benson CH. Water content-density criteria for compacted soil liners. Journal of Geotechnical Engineering 1990; 116:1811–1830. https://doi.org/10.1061/(ASCE)0733-9410(1990)116:12(1811)

[38] Mitchell JK, McConnell JR. Some Characteristics of the elastic and plastic deformation of clay on initial loading. Institute of Transportation and Traffic Engineering, University of California 1965.

[39] Watabe Y, Leroueil S, le Bihan J-P. Influence of compaction conditions on pore-size distribution and saturated hydraulic conductivity of a glacial till. Canadian Geotechnical Journal 2000; 37:1184–1194. https://doi.org/10.1139/t00-053

[40] Mitchell JK, Hooper DR, Campenella RG. Permeability of compacted clay. Journal of the Soil Mechanics and Foundations Division 1965; 91:41–65.

[41] Ranaivomanana H, Razakamanantsoa A, Amiri O. Effects of cement treatment on microstructural, hydraulic, and mechanical properties of compacted soils: Characterization and modelling. International Journal of Geomechanics 2018; 18:04018106. https://doi.org/10.1061/(ASCE)GM.1943-5622.0001248

[42] Ranaivomanana H, Razakamanantsoa A, Amiri O. Permeability prediction of soils including degree of compaction and microstructure. International Journal of Geomechanics 2017; 17:04016107. https://doi.org/10.1061/(ASCE)GM.1943-5622.0000792

[43] González-López JR, Juárez-Alvarado CA, Ayub-Francis B, Mendoza-Rangel JM. Compaction effect on the compressive strength and durability of stabilized earth blocks. Construction and Building Materials 2018; 163:179–188. https://doi.org/10.1016/j.conbuildmat.2017.12.074

[44] Holtz RD, Kovacs WD, Sheahan TC. An introduction to geotechnical engineering, Prentice-Hall Englewood Cliffs, NJ 1981.

[45] Kouassi P, Breysse D, Girard H, Poulain D. A new technique of kneading compaction in the laboratory. Geotechnical Testing Journal 2000; 23:72–82. https://doi.org/10.1520/GTJ11125J

[46] Williams FHP. Compaction of Soils. Journal of the Institution of Civil Engineers 1949; 33:73–99

[47] Russ DH. Anisotropic properties of compacted silty clay Ohio University Library. 1996.

[48] Lekarp F, Isacsson U, Dawson A. State of the art. II: Permanent strain response of unbound aggregates. Journal of Transportation Engineering 2000; 126:76–83. https://doi.org/10.1061/(ASCE)0733-947X(2000)126:1(76)

[49] Lutenegger AJ. Soils and Geotechnology in Construction. CRC Press; 2019.

[50] le Vern M, Sediki O, Razakamanantsoa A, Murzyn F, Larrarte F. Experimental study of particle lift initiation on roller-compacted sand–clay mixtures. Environmental Geotechnics 2020:1–12. https://doi.org/10.1680/jenge.19.00172

[51] Clegg B. Kneading compaction. Australian Road Research Board Bulletin 1964; 1.

[52] Cherian C, Arnepalli DN. A critical appraisal of the role of clay mineralogy in lime stabilization. International Journal of Geosynthetics and Ground Engineering 2015; 1.

[53] ASTM standard D 6276-99a. Standard Test Method for Using pH to Estimate the Soil–Lime Proportion Requirement for Soil Stabilization. American Society for Testing and Materials 2006.

[54] ASTM A, D698-12e2. Standard Test Methods for Laboratory Compaction Characteristics of Soil Using Standard Effort (12 400 Ft-Lbf/Ft3 (600 KN-m/M3)) 2012.

[55] GTS - LCPC-Setra Technical Guide. Soil treatment with lime and/or hydraulic binders: Application to the Construction of fills and capping layers. LCPC Eds, Paris (France) 2000.

[56] Barrett EP, Joyner LG, Halenda PP. The determination of pore volume and area distributions in porous substances. I. Computations from nitrogen isotherms. Journal of the American Chemical Society 1951; 73:373–380. https://doi.org/10.1021/ja01145a126

[57] Lei XY. Pore distribution characteristics of Long-dong loess in Northern Shanxi of China, Chin. Sci. Bull 1985; 30:206–209.

[58] Wang M, Bai X-H, Liang R, CHEN P. Microstudy on soft foundations reinforcement with lime-fly ash piles, Rock and Soil Mechanics-WUHAN 2001; 22:67–70.

[59] Bin S, Zhibin L, Yi C, Xiaoping Z. Micropore structure of aggregates in treated soils. Journal of Materials in Civil Engineering 2007; 19:99–104. https://doi.org/10.1061/(ASCE)0899-1561(2007)19:1(99)

[60] Romero E, Simms PH. Microstructure investigation in unsaturated soils: a review with special attention to contribution of mercury intrusion porosimetry and environmental scanning electron microscopy. Geotechnical and Geological Engineering 2008; 26:705–727.

[61] Brunauer S, Emmett PH, Teller E. Adsorption of gases in multimolecular layers. Journal of the American Chemical Society 1938; 60:309–319.

[62] Westermarck S. Use of mercury porosimetry and nitrogen adsorption in characterisation of the pore structure of mannitol and microcrystalline cellulose powders, granules and tablets 2000.

[63] Rouquerol J, Avnir D, Fairbridge CW, Everett DH, Haynes JM, Pernicone N, Ramsay JDF, Sing KSW, Unger KK. Recommendations for the characterization of porous solids (Technical Report), Pure and Applied Chemistry 1994; 66:1739–1758.

[64] Lemaire K, Deneele D, Bonnet S, Legret M. Effects of lime and cement treatment on the physicochemical, microstructural and mechanical characteristics of a plastic silt. Engineering Geology 2013; 166:255–261. https://doi.org/10.1016/j.enggeo.2013.09.012

[65] Nguyen TTH. Stabilisation des sols traités à la chaux et leur comportement au gel. 2015.

[66] Sotomayor FJ, Cychosz KA, Thommes M, Characterization of micro/mesoporous materials by physisorption: concepts and case studies, Accounts of Materials & Surface Research 2018; 2:36-37.

[67] McGregor F, Heath A, Fodde E, Shea A. Conditions affecting the moisture buffering measurement performed on compressed earth blocks. Building and Environment 2014; 75:11–18. https://doi.org/10.1016/j.buildenv.2014.01.009

[68] Collet F, Bart M, Serres L, Miriel J. Porous structure and water vapour sorption of hemp-based materials. Construction and Building Materials 2008; 22:1271–1280. https://doi.org/10.1016/j.conbuildmat.2007.01.018

[69] Zielinski JM, Kettle L. Physical characterization: surface area and porosity. London: Intertek 2013.

[70] Verbrugge J-C, de Bel R, Correia AG, Duvigneaud P-H, Herrier G. Strength and micro-observations on a lime treated silty soil, in: Road Materials and New Innovations in Pavement Engineering 2011:89–96. https://doi.org/10.1061/47634(413)12

[71] Ajayi ES. Effect of Lime Variation on the Moisture Content and Dry Density of Lateritic Soil in Ilorin, Nigeria. 2012.

[72] Consoli NC, Prietto PDM, da Silva Lopes Jr L, Winter D. Control factors for the long term compressive strength of lime treated sandy clay soil. Transportation Geotechnics 2014;1:129–36. https://doi.org/10.1016/j.trgeo.2014.07.005

[73] Yin C, Zhang W, Jiang X, Huang Z. Effects of initial water content on microstructure and mechanical properties of lean clay soil stabilized by compound calcium-based stabilizer. Materials 2018;11:1933. https://doi.org/10.3390/ma11101933

[74] Kichou Z, A study on the effects of lime on the mechanical properties and behaviour of London clay 2015 (Doctoral dissertation, London South Bank University).

[75] Tran TD, Cui Y-J, Tang AM, Audiguier M, Cojean R. Effects of lime treatment on the microstructure and hydraulic conductivity of Héricourt clay. Journal of Rock Mechanics and Geotechnical Engineering 2014; 6:399–404. https://doi.org/10.1016/j.jrmge.2014.07.001

[76] Wang D, Zentar R, Abriak NE. Temperature-accelerated strength development in stabilized marine soils as road construction materials. Journal of Materials in Civil Engineering 2017; 29:04016281. https://doi.org/10.1061/(ASCE)MT.1943-5533.0001778

[77] Charles I, Herrier G, Chevalier C, Durand E. An experimental full-scale hydraulic earthen structure in lime treated soil. 6th International Conference on Scour and Erosion, Paris, 2012, p. 1223–30.

[78] ASTM-C42-77. Standard method of obtaining and testing drilled cores and sawed beams of concrete. American Society for Testing and Materials, West Conshohocken, PA, USA 1978.